Error Estimations of 3D Digital Image Correlation Measurements

Introduction

Digital image correlation as a tool for surface deformation measurements has found widespread use and acceptance in the field of experimental mechanics. The method is known to reconstruct displacements with subpixel accuracy and tangential surface strains in the sub-milliStrain range. Potential error sources, limiting the system resolution, are versatile, as there are e.g. intrinsic noise of the acquired images, statistical and systematical errors introduced by the system calibration, subpixel effects resulting from a limited camera resolution [2], as well as intrinsic uncertainties of the correlation algorithm. The impact on resulting quantities like contours, displacements and strains depends essentially on the nature of the error source. A statistical, i.e. random error distribution can be estimated from the results themselves, and the quality of the result can be further improved by proper filtering.
Contrary to this systematical errors, as they are introduced by an erroneous system calibration, cannot be reduced by post-processing and thus build a hard limit for the system resolution.

In 2005 we introduced a commercial 3D image correlation system Q-400 [4]. It is used in a widespread field of applications as e.g. in automotive, aerospace and research fields. The system provides a smart calibration tool with an online feedback of the calibration quality. It is capable of estimating the uncertainties of the resulting calibration parameters. In addition the system gives uncertainties of the evaluated displacements and strains as a result of the image correlation algorithm. We run performance tests in order to get an understanding of the impact of correlation and calibration errors and to determine the resolution limit of the system. Here we present some of the results:

Fig.1: Performance Test of the Q-400 system: A glass plate, sprayed with a stochastic speckle pattern, is mounted on a translation stage and is moved successively in horizontal in-plane direction by a known distance. After each step a measurement with the Q-400 system is done. A full field analysis of the measured displacements and strains, provides information about present calibration errors.

FOV: 13x9 cm^2
Cameras: JAI-A1 CCD camera with 1392x1040 pixels
Lenses: Schneider-Kreuznach, focal lengths 4.8, 17 and 50mm
Displacement range: 0-46mm, reference accuracy: 1µm
Lightning: HiLis [4], multi LED-illumination, $\lambda = 520 - 550nm$,
optimized for bright and homogeneous illumination conditions.

Outline of Digital Image Correlation

In the 3D digital image correlation technique, random gray-value dot patterns on specimen surfaces are observed by two cameras in a stereoscopic setup (Fig. 1). The digitized images are compared to match subsets – so called *facets* - from one image to another by using an image correlation algorithm. Typically a facet size between 20x20 and 30x30 pixels is chosen. With knowledge of the imaging parameters for each camera and the orientations of the cameras with respect to each other, the position of each object point in three dimensions is calculated. In order to evaluate surface displacements and strains on the object surface, a series of measurements is taken, while the specimen surface is moved due to a loading. The correlation algorithm tracks the observed gray value patterns for each camera and transforms corresponding facet positions in both cameras into 3D coordinates for each step, resulting in a track of each surface facet in 3D space. As the surface deformation is measured pointwise, displacements of individual surface points, and subsequently surface strains can be evaluated.
The correlation algorithm is based on a pseudo-affine coordinate transformation from one camera image to another:

$$x_t(a_0, a_1, a_2, a_3, x, y) = a_0 + a_1 x + a_2 y + a_3 xy$$
$$y_t(a_4, a_5, a_6, a_7, x, y) = a_4 + a_5 x + a_6 y + a_7 xy$$

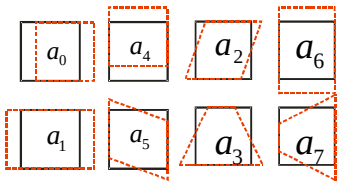

The possible transformations consist of a combination of translations, stretch, shear and distortion.

Within the correlation algorithm the transformation parameters are determined by minimizing the distance between the observed gray value pattern $G_2(x\ ,y\ )$ in the second image and the original pattern $G_1(x, y)$ by applying the coordinate transformations (x_t, y_t) plus photogrametric corrections, which consider different contrast and intensity levels of the images:

$G_T(x, y) = g_0 + g_1 G_2(x_t(x, y), y_t(x, y))$ and

$$\min_{a_0,\ldots,a_7,g_0,g_1} \sum_{x,y} \left\| G_1(x, y) - G_T(x, y) \right\|$$

System Calibration

The calibration procedure is part of the acquisition module of the measurement system. Its purpose is the determination of the imaging parameters of each of the cameras (intrinsic parameters) as well as the external positions and orientations of the cameras with respect to a global coordinate system. The system calibration is needed for transforming image positions on the CCDs of the two cameras of a specimen surface point to the corresponding 3D coordinates of that point. Calibration errors are potentially a major source of systematic evaluation errors limiting the resolution of the results.
The calibration algorithm makes use of the “Plumb Model”, introduced by Brown (1966) [1]. According to this model the projection of the object point on the CCD is defined by the intersection of the line from the object point through the principle point and the CCD (pinhole model, see Fig. 2). The distance of the principle point to the image plane is the focal length f, the projection on the image plane gives the position of the optical axis on the CCD. Every deviation from the straightness of the projection can be related to the presence of radial (α_r) and tangential (α_t) distortion:

$$\tilde{P} = (1 + \alpha_r)P + \alpha_t,$$

where P is the projected point according to the plain pinhole model, $\tilde{P}$ is the distorted point.
The amount of the radial distortion can be expressed in the following form:

$$\alpha_r = \alpha_2 r^2 + \alpha_4 r^4 + \ldots$$

The present calibration algorithm evaluates the radial distortion up to the 4th order: $\alpha_r = \alpha_2 r^2 + \alpha_4 r^4$.

Tangential distortions occur as a fact of misalignment of lenses. In general they are small compared to the radial distortions. Tangential distortions can be described as follows:

$$\alpha_t = \begin{pmatrix} 2t_x xy + t_y(r^2 + 2x^2) \\ t_x(r^2 + 2y^2) + 2t_y xy \end{pmatrix}$$

with tangential distortion parameters t_x, t_y.

The calibration is done by taking a series of exposures of a calibration target with both cameras simultaneously. The calibration target is a chess pattern with known geometry. The software detects the corners of the squares. Additional circular markers define the center and the orientation of the target. During the calibration process these markers are detected automatically and displayed online on the monitor, while the calibration target is positioned into different spatial orientations. The evaluation algorithm calculates the intrinsic parameters (focal length, principle point, distortion parameters) for each camera, the extrinsic parameters (translation vector and rotation matrix) as well as the uncertainties of the calibration parameters, resulting from the deviations of the detected markers from the model positions. Typically a total number of eight images are sufficient to calculate all calibration parameters accurately.

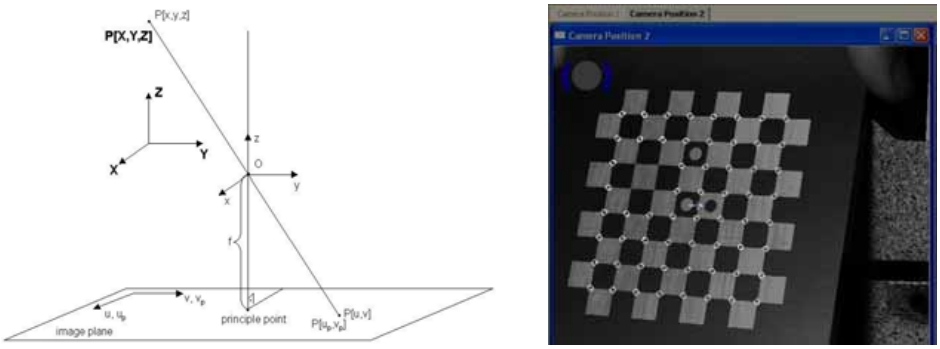

Fig. 2: Illustration of the camera calibration procedure.
***Left:** Pinhole model (ignoring distortion**), **Right:** automatic search of the markers on the calibration target.*

Error Classifications

The evaluation of a 3D correlation measurement results in 3D coordinates, surface displacements and tangential strains of the specimen's surface. The corresponding data uncertainties originate from different sources, which can be divided into two categories according to their impact on the evaluation process: Error sources, which influence the accuracy of the image correlation, are called *correlation errors*, contrary to calibration errors, which have a direct impact on the reconstruction of the 3D coordinates of correlated image facets, we call them *3D reconstruction errors*. In the following paragraphs both error groups are discussed separately:

Correlation Error:

Correlation errors describe uncertainties for the correlation of corresponding facet positions in different image frames. Correlation errors can be divided in statistical and systematical errors. Statistical errors occur first of all because of the limited number of pixels and corresponding gray values in each facet, and the fact, that the facet position has to be determined with subpixel accuracy. The corresponding statistical error decreases with the square root of the number of facet pixels. Additional potential error sources are statistical noise of the gray values, different illumination conditions for the two cameras, image contrast and size of the speckle pattern on the specimen surface.
Systematical errors are introduced by subpixel effects, which occur because of the discretization of the real speckle pattern by the CCD pixels, and potentially by a non-linear distortion of the facets, if the linear facet transformation model does not match, e.g. for a curved specimen surface or for significant camera distortions. Statistical errors can be minimized by smoothing operations or by adding up a few frames. Systematical errors such as an unsufficient correlation model build a principal limitation for the resolution of the resulting data. This effect can be demonstrated by the comparison of the evaluation of a sphere and a plane (Fig. 3). The plotted graphs show the correlation error, which is provided by the system in dependence of the chosen facet size. Both measurements are done under identical conditions with a camera field of view of 13x9 cm^2, whereas the sphere's diameter amounts 7.3cm. For small facet sizes the correlation error for sphere and plane are identical and follow the statistical uncertainties according to the number of facet pixels. With increasing facet sizes systematical errors appear, thus for the plane the correlation error does not diminish any more, if the facet size is greater than 80 pixels, for the sphere a minimal correlation error occurs for a facet size of 50 pixels and increases again for larger facet sizes due to the curvature of the sphere surface.

3D coordinates reconstruction error:

Uncertainties of the calibration parameters lead to errors, when reconstructing the 3D coordinates from correlated facets of the two cameras. Calibration errors appear in a systematical manner as a function of the facet positions in the camera frames, causing local distortions of the reconstructed 3D space. In order to get an understanding of the impact on the evaluated data, the distortion effects can be described by the following formalism:
Be $P = (x, y, z)$ the real position of a reconstructed point. The measured coordinate $\tilde{P}$ differs from P by a deviation vector ΔP. In the vicinity of a point $P_0 = (x_0, y_0, z_0)$ the error vector can be written as:

$$\Delta P(P_0 + \vec{r}) = \Delta P(P_0) + \vec{\vec{k}} \cdot \vec{r} \,,$$

$$\vec{\vec{k}} = (\vec{k}_x, \vec{k}_y, \vec{k}_z) = \begin{pmatrix} k_{xx} & k_{xy} & k_{xz} \\ k_{yx} & k_{yy} & k_{yz} \\ k_{zx} & k_{zy} & k_{zz} \end{pmatrix}$$

with a distortion matrix $\vec{\vec{k}}$. As a consequence the displacement v of a point, which moves from the coordinate $P_1 = (x_1, y_1, z_1)$ to $P_2 = (x_2, y_2, z_2)$, is measured as: $\tilde{v} = (\vec{\vec{1}} + \vec{\vec{k}}_0) \cdot v$.

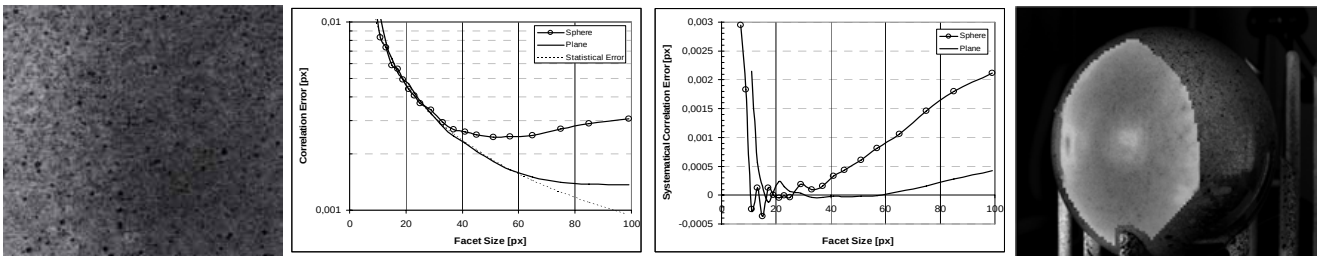

Fig. 3: Correlation Errors, provided by the measurement system for the evaluation of a plane and of a sphere as a function of facet size. The images show the correlation error distribution in the evaluated area, where a bright colour indicates a larger uncertainty. As can be seen in the right image, the correlation error increases towards the boarder of the evaluation area of the sphere, caused by larger perspective distortions of the facets in camera 2 with respect to camera 1. At the center a local maximum of the correlation error is revealed. This is caused by a little reflex of the illumination in one of the cameras.

Left plot: *The dashed line represents the theoretical statistical error according to the number of facet pixels. A minimal correlation error of 0.0014px occurs for the plane, corresponding sphere errors are 0.0024px. The correlation errors translate into 3D coordinate uncertainties according to the projected camera pixel size (for the present setup: 0.16µm for the plane, 0.28µm for the sphere). The corresponding displacement errors amount 0.22µm (0.39µm). The uncertainties of the strain data, deduced by the 3D coordinates and the surface displacements, depend on the baselength, i.e. the distance of neighbouring points of the surface points. If the baselength is chosen identical to the facet size, which makes sense, because the facet size determines the spatial resolution, the strain error is reduced continuously with increasing facet size for the plane as well as for the sphere measurement down to 0.2(0.5) mStrain for the largest evaluated facet.*

Right Plot: *Difference between total correlation error and theoretical statistical error. For high facet sizes the curves can be interpreted as systematic errors caused by facet distortions. For low facet sizes a significant drop of the correlation quality can be observed, if the facet size falls below 15 pixels.*

In general $\vec{\vec{k}}$ is a function of the position in space. Thus the displacements must be written as:

$$\tilde{v} = \tilde{P}_2 - \tilde{P}_1 = v + \int_{x_1}^{x_2} \vec{k}_x dx + \int_{y_1}^{y_2} \vec{k}_y dy + \int_{z_1}^{z_2} \vec{k}_z dz \,.$$

We measured three components $\vec{k}_x$ of the distortion matrix directly with a correlation system by successively moving a plane plate into the x-direction (i.e. horizontal in-plane direction, see Fig. 1) and comparing the evaluated displacements in the three coordinate directions with respect to a reference. The total field of view was 13x9 cm^2. The experiment showed that up to a displacement of 50 CCD pixels (i.e.5mm on the specimen's surface), the displacement errors increase linearly, as expected by the "constant $\vec{\vec{k}}$" approach. Thus $\vec{k}_x$ can be evaluated by

$$\vec{k}_x = (\tilde{v} - v)/\|v\| \quad \text{with } \|v\| < 5mm \,.$$

Fig. 5 displays the spatial distribution of the distortion coefficients over the field of view for three different camera lenses with focal lengths of 4.8mm, 17mm and 50mm. While for the 17mm and 50mm lenses the distortion coefficients show systematical displacement errors of a similar magnitude in a range of 0.01-0.05%, relative to the real displacement, the measurement results show significantly larger displacement errors for the 4.8mm lens up to 3%. k_{xx} shows a circular distribution, with increasing amplitudes towards the boarder of the field of view, indicating, that the used calibration model is not anymore capable of matching the significant radial distortions, which are present, when using extreme wide angle lenses. This interpretation is strengthened by the fact, that the circular structures are reproducible by different calibrations. As a practical result, the useful area is restricted to the central circular region with a diameter of less than 50% of the FOV, where the distortion values are only slightly higher than the ones for the other lenses. With increasing focal length the systematic effect vanishes and the distortion coefficients are dominated by the statistical uncertainties of the calibration measurement.

In the case of a locally constant distortion matrix, strains, which are measured through the relative displacements of nearby points of a specimen surface, are unaffected, as $\vec{\vec{k}}$ acts on the displacements the same way as it does on the measurement of the base length. For the 4.8mm lens, the distortion vector shows significant gradients, thus the lokal "constant k" assumption is not anymore valid. Assume, a local strain is computed by the relative displacements of two neighbouring points on the specimen's surface, which are separated by a distance l.

Using a 1.order approximation of

$\vec{k}_x(x,y,z) = \vec{k}_{x,0} + Dk_x \cdot (x,y,z)^T$ with the Jacobian matrix of $\vec{k}_x$, $Dk_x = \left(D\vec{k}_x{}^x, D\vec{k}_x{}^y, D\vec{k}_x{}^z\right)$,
a displacement into x-direction $\vec{v} = (v_x, 0, 0)$ is measured as:

$$\tilde{\vec{v}} = (\vec{1} + \vec{k}_{x,0}) \cdot v_x + \frac{1}{2} D\vec{k}_{x,0}{}^x \cdot v_x{}^2,$$

leading to a normal strain measurement in x-direction of:

$$\tilde{\varepsilon}_{xx} = \varepsilon_{xx} + D\vec{k}_x{}^{xx} \cdot v_x + \frac{1}{2}\varepsilon_{xx} \cdot D\vec{k}_x{}^{xx} \cdot l,$$

where v_x is a local rigid body movement in x-direction,
$D\vec{k}_x{}^{xx}$ is the first component of $D\vec{k}_x{}^x$.

Thus rigid body movements as well as present strains lead to systematical errors of the strain measurement in the presence of distortion gradients, which increase linearly with the rigid body motions and the present strain. Table 1 lists the evaluated distortion components of the displacement measurements for the three used lenses. The measurements show significantly less strain errors for the 50mm lens, the reason is the smoother spatial distribution of the distortion matrix, leading to lower gradients and, as a consequence to lower strain errors.

Lens	k_{xx} / [10^{-3}]			k_{xy} / [10^{-3}]			k_{xz} / [10^{-3}]			$D\vec{k}_x{}^{xx}$ / [10^{-6}/px]		
	min	**max**	**center**	**min**	**max**	**center**	**min**	**max**	**center**	**min**	**max**	**center**
4.8mm total frame	-31.1	2.8	0.56	-19.5	0.9	-0.14	-17.2	11.9	0.24	-500	23	1.3
4.8mm central region	-0.14	0.66		-0.52	0.16		-0.22	1.80		-5.3	5.1	
17mm	-0.46	0.46	0.060	-0.21	0.21	-0.026	-0.38	0.38	0.071	-3.3	4.4	-1.8
50mm	-0.26	0.26	0.087	-0.13	0.26	-0.011	-0.17	0.12	0.034	-1.3	1.5	3.8

Table 4: Minimal and Maximal distortion coefficients for the displacement measurements of three different lenses.

	k_{xx}	k_{xy}	k_{xz}	$D\vec{k}_x{}^{xx}$
Focal Length: 4.8mm Gray Scale Range: k = -10^{-3} - $+10^{-3}$ Gray Scale Range : $D\vec{k}_x{}^{xx}$ = -0.1 - +0.1/px	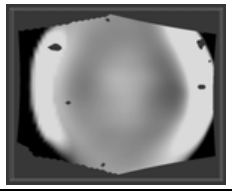	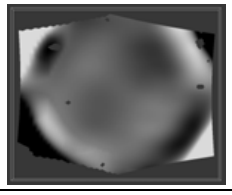	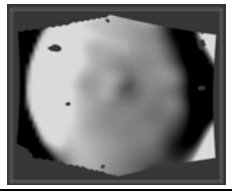	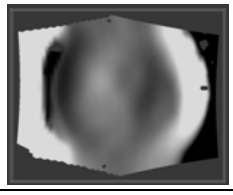
Focal Length: 17mm Gray Scale Range: k = $-0.3\cdot10^{-3}$ - $+0.3\cdot10^{-3}$ Gray Scale Range : $D\vec{k}_x{}^{xx}$ = -0.1 - +0.1/px	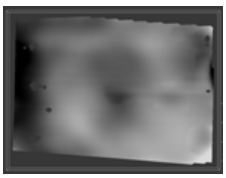	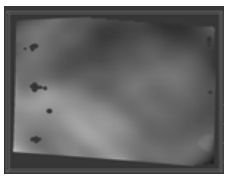	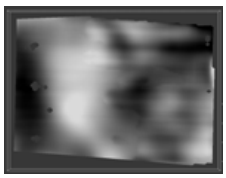	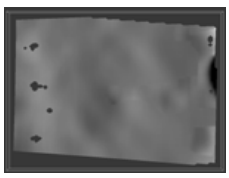
Focal Length: 50mm Gray Scale Range: k=$-0.2\cdot10^{-3}$ - $+0.2\cdot10^{-3}$ Gray Scale Range : $D\vec{k}_x{}^{xx}$=-0.1 - +0.1/px	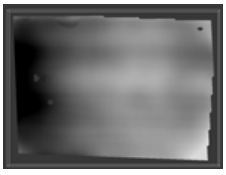		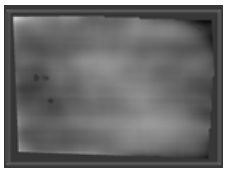	

Fig 5: Spatial distribution of the distortion coefficients for the displacement measurements of three different lenses.

Summary

We presented results of performance tests of a digital image correlation system for full field displacement and strains measurements on a specimen's surface. It could be shown that calibration errors introduce systematic errors on the resulting data. Displacement errors are present in the order of less than 0.02px, strain errors are limited to 0.05mStrain, when using a lens with 50mm focal length, or 0.2mStrain for a 17mm lens, even for large displacements of about 25% of the field of view. If present displacements are small (lower than 50px), the errors scale linearly. Relative displacement errors are in the order of 0.01-0.05%, strain errors typically count 1-5µStrain/px, related to the existent displacements. One exception is found by the results of an extreme wide angle lens with a focal length of 4.8mm. In that case present camera distortions break the assumptions of the calibration model, leading to systematical calibration errors. It needs to be stated that this wide angle lens represents an extreme setup, that has limited relevance for the majority of all practical applications. Nevertheless our claim for future system developments is to extend the model of radial distortions to an additional term and thus to reduce the systematical calibration errors even more.

References

1. Brown, D.C. (1966), ”Decentering distortion of lenses“, Photogrammetric Engineering, 32(3), 444-462
2. Schreier, H.W., Braasch, J.R., Sutton, M.A. (2006), “Systematic errors in digital image correlation caused by intensity imterpolation“, Opt. Eng. 39(11), 2915-2921
3. Yoneyama, S., Kikuta, H. (2006), ”Lens distortion correction for digital image correlation.“, Opt. Eng. 45(2)
4. Digital 3D-Correlation System Q-400, http://www.dantecdynamics.com

Authors:

Thomas Becker,
Karsten Splitthof,
Thorsten Siebert,
Peter Kletting
Dantec Dynamics GmbH, Germany

Copy of a paper presented at:
The International Conference Speckle06
“Speckles, From Grains to Flowers”
Nimes, France (13.-15. Sept. 2006)

Fore more information, please contact:

Dantec Dynamics GmbH
Kaessbohrerstraße 18
D-89077 Ulm

Tel.: +49-731-9332200
Fax: +49-731-9332299

E-mail: product.support@dantecdynamics.com
Internet: http://www.dantecdynamics.com